

# Krypton in presolar mainstream SiC grains from AGB stars

M. Pignatari<sup>1</sup>, R. Gallino<sup>1,2</sup>, S. Amari<sup>3</sup> and A.M. Davis<sup>4</sup>

<sup>1</sup> Dipartimento di Fisica Generale, Università di Torino, via P. Giuria 1, 10125 Torino, Italia  
e-mail: pignatar@ph.unito.it

<sup>2</sup> Centre for Stellar and Planetary Astrophysics, School of Mathematical Sciences, Building 28, Monash University, Victoria 3800, Australia

<sup>3</sup> Laboratory for Space Sciences and the Physics Department, Washington University, St. Louis (MO 63130, USA)

<sup>4</sup> Enrico Fermi Institute and Dept. of the Geophysical Sciences, University of Chicago, Chicago (IL 60637, USA)

**Abstract.** Presolar mainstream SiC grains condensed in the circumstellar envelopes of AGB stars. The isotopic composition of trace elements present in SiC shows the characteristic signature of the *s*-process. In this work we present an analysis of the krypton-*s* component using AGB model predictions and discuss the most recent implantation scenarios of noble gases. Nuclear uncertainties affecting our results are discussed, with particular emphasis to the branching points of <sup>79</sup>Se and <sup>85</sup>Kr.

## 1. Introduction

When low mass stars evolve along the Asymptotic Giant Branch phase (AGB), carbon and *s*-process elements freshly synthesised in the He-intershell are mixed in the envelope by third dredge-up events (Straniero et al. 1997). Late on the AGB the stellar envelope becomes carbon-rich ( $C/O > 1$ ), the necessary condition for the formation of SiC grains (Zinner 1998).

Noble gases do not condense in dust, but need to be ionised and implanted. Two different regimes have been proposed: a *cold* and partially ionised wind in the mass losing envelope and a *hot* and fully ionised wind

at higher energy, during the planetary nebula phase (Lewis et al. 1990; Gallino et al. 1990; Verchovsky et al. 2004). Regarding Xe, Pignatari et al. (2004) analysed the Xe-G component (the pure *s*-component) in mainstream SiC grains. In that paper, it was shown that  $(^{134}\text{Xe}/^{130}\text{Xe})_G$  is an indicator of the implantation mechanism: the observed ratio is better reproduced by the cold implantation scenario. This is in agreement with the evidence of a chemical fractionation between the heavy and the light noble gases (Lewis et al. 1990, 1994) and also with analysis of the xenon implantation energy in the grains (Verchovsky et al. 2004). In this paper we want to analyse the Kr-G component in mainstream SiC grains. For a detailed description of the *s*-process in AGB stars see Gallino et al. (1998). In §2 we briefly describe the *s* nucleosynthesis of kryp-

---

Send offprint requests to: M. Pignatari

Correspondence to: Dipartimento di Fisica Generale, via P. Giuria 1, 10125 Torino, Italy

ton isotopes; in §3 the Kr–G component in mainstream SiC grains is discussed and in §4 it is compared with predictions from AGB stellar models; In §5 we present the main conclusions of this work.

## 2. Krypton–S

The lightest Kr isotope,  $^{78}\text{Kr}$ , is  $p$ -only and is destroyed by the  $s$ -process.  $^{80}\text{Kr}$  and  $^{82}\text{Kr}$  are  $s$ -only (with a non negligible  $p$ -process contribution), shielded against the  $r$ -process by the respective stable isobars  $^{80}\text{Se}$  and  $^{82}\text{Se}$ . The  $^{80}\text{Kr}$  nucleosynthesis depends on the branching of unstable  $^{79}\text{Se}$ . For the  $\beta^-$  decay rate at stellar conditions we follow the prescriptions of Klay & Käppeler (1988), while for the neutron capture cross section we use the Bao et al. (2000) recommended rate. Both rates suffer from a quite large uncertainty. A typical  $s$ -process odd–even pattern is predicted for  $^{82}$ – $^{84}\text{Kr}$  isotopes.  $^{86}\text{Kr}$  is a neutron magic isotope ( $N = 50$ ). For this reason, its neutron capture cross section is particularly low ( $4.737 \pm 0.021$  mb, 30 keV). Its production by the  $s$ -process depends on the  $^{85}\text{Kr}$  neutron channel.  $^{85}\text{Kr}$  is an unstable isotope, characterised by a ground state,  $^{85}\text{Kr}^g$  ( $t_{1/2} = 10.76$  yr), and an isomeric state,  $^{85}\text{Kr}^m$  ( $t_{1/2} = 4.48$  h). About 50 % of the neutron capture of  $^{84}\text{Kr}$  feeds  $^{85}\text{Kr}^m$  (Bao et al. 2000). According to Ward et al. (1976), for  $T_9 < 0.3$  (expressing temperature in units of  $10^9$  K)  $^{85}\text{Kr}^g$  and  $^{85}\text{Kr}^m$  are not thermalised and must be considered as two separate nuclear species. The ground and the isomeric states decay with their terrestrial rates. 20% of  $^{85}\text{Kr}^m$  suffers from a  $\gamma$  internal transition to the ground state,  $^{85}\text{Kr}^g$ , whereas the remaining 80%  $\beta^-$ -decays to  $^{85}\text{Rb}$ .

For  $^{80}\text{Kr}$ ,  $^{82}$ – $^{84}\text{Kr}$  and  $^{86}\text{Kr}$ , we use the neutron capture cross sections by Mutti et al. (2005). For the unstable isotopes  $^{81}\text{Kr}$  and  $^{85}\text{Kr}$  we use the theoretical neutron capture cross sections recommended by Bao et al. (2000), which again suffer from a quite large uncertainty.

## 3. Kr–G in mainstream SiC grains

In Fig. 1 the krypton isotopic ratios for the G–component extrapolated by Lewis et al.

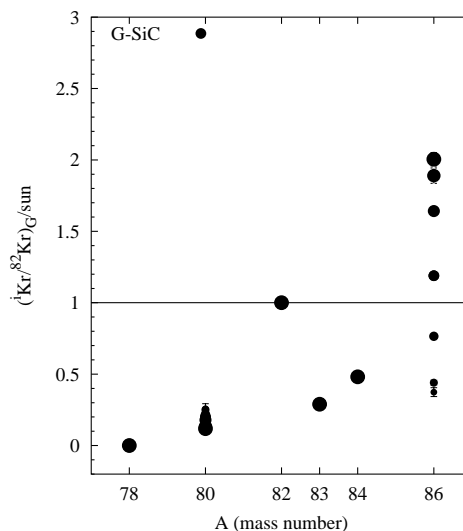


**Fig. 1.** Kr–G isotopic ratios measured in mainstream SiC grains (black circles, data from Lewis et al. 1994) are plotted for different grain size separates, from the smallest (KJA, small circles) to the largest (KJG, big circles).

(1994) from different grain size separates (each separate is made of  $10^5$ – $10^6$  grains) are plotted normalised to solar (Lodders 2003). The  $(^{86}\text{Kr}/^{82}\text{Kr})_G$  ratio strongly increases with the grain size. The  $(^{80}\text{Kr}/^{82}\text{Kr})_G$  ratio, instead, slightly decreases. We observe that  $^{80}\text{Kr}$  and  $^{82}\text{Kr}$  are  $s$ -only, so one would naively expect the  $(^{80}\text{Kr}/^{82}\text{Kr})_s$  normalised to solar be close to one. However, solar  $^{80}\text{Kr}$  is produced by the main  $s$ -component in AGB stars by only 12 %, while the residual 88 % derives from the weak  $s$ -process in massive stars. Regarding solar  $^{82}\text{Kr}$ , 37 % derives from the main  $s$ -component while 63 % from the weak  $s$ -component (Arlandini et al. 1999, Pignatari et al. 2005a). Presolar SiC grains offer a unique observational opportunity to confirm the above expectation, with the isotopic ratio  $(^{80}\text{Kr}/^{82}\text{Kr})_G$  normalised to solar being pretty close to  $0.12/0.37 = 0.3$ .

In Fig. 7 of Lewis et al. (1994),  $(^{86}\text{Kr}/^{82}\text{Kr})_G$  and  $^{86}\text{Kr}/^{82}\text{Kr}$  (the isotopic ratio directly measured in the SiC grains) for different grain sizes are plotted with respect to  $(^{130}\text{Xe}/^{82}\text{Kr})_G$  and  $^{130}\text{Xe}/^{82}\text{Kr}$ , respectively.

In fine grains, the  $^{130}\text{Xe}/^{82}\text{Kr}$  ratio is  $\sim 2.5$ , whereas in coarse SiC grains is  $\sim 0.2$ . In the AGB envelope and in the He–intershell  $^{130}\text{Xe}/^{82}\text{Kr}$  reaches *at most* 0.2. A chemical fractionation Xe/Kr due to a partial gas ionization has been proposed as an explanation of the high values measured in fine grains. To explain the  $(^{86}\text{Kr}/^{82}\text{Kr})_G$  spread, Lewis et al.

(1994) suggested two possible scenarios. (i) Fine grains form in the C–rich envelope during early thermal pulses, when  $^{86}\text{Kr}/^{82}\text{Kr}$  is low and the wind temperature lets  $^{130}\text{Xe}/^{82}\text{Kr}$  be high enough. Coarse grains progressively condense in the following pulses, where the  $^{86}\text{Kr}/^{82}\text{Kr}$  ratio progressively increases. (ii) SiC grains of different size form in the envelope of AGB stars of different metallicities. Coarse grains condense in low metallicity AGB stars, where a high  $^{86}\text{Kr}/^{82}\text{Kr}$  is predicted. A hot and unfractionated implantation wind could explain the low  $^{130}\text{Xe}/^{82}\text{Kr}$  in coarse grains. AGB stars with solar–like metallicity produce the fine grains with low  $^{86}\text{Kr}/^{82}\text{Kr}$ . A cold and fractionated wind could explain the high  $^{130}\text{Xe}/^{82}\text{Kr}$  in fine grains. The results by Pignatari et al. (2004) seem to disagree with the second scenario. The Xe–G component in mainstream SiC grains does not agree with AGB models predictions at low metallicity ( $Z \leq 1/3 Z_\odot$ ), because the  $(^{134}\text{Xe}/^{130}\text{Xe})_s$  ratio is too high with respect to the observed one. Using an analytical model of implantation of Kr in grains of different sizes for different kinetic energies, Verchovsky et al. (2004) showed that, whereas  $^{86}\text{Kr}$ –G is implanted mainly by hot winds,  $^{82}\text{Kr}$ –G is affected by both the cold and the hot components. This implies that the low  $(^{86}\text{Kr}/^{82}\text{Kr})_G$  in fine grains (KJA, KJB and KJC samples, see Verchovsky et al. 2004, Fig. 3) is an effect of the low implantation energy for the two isotopes. In coarse SiC grains (KJD, KJE and KJF) both  $^{86}\text{Kr}$  and  $^{82}\text{Kr}$  are instead implanted by hot winds.

#### 4. Comparison of Kr–G in SiC grains and AGB models

To reproduce the Kr–G component in the hot implantation scenario, we base our analysis on

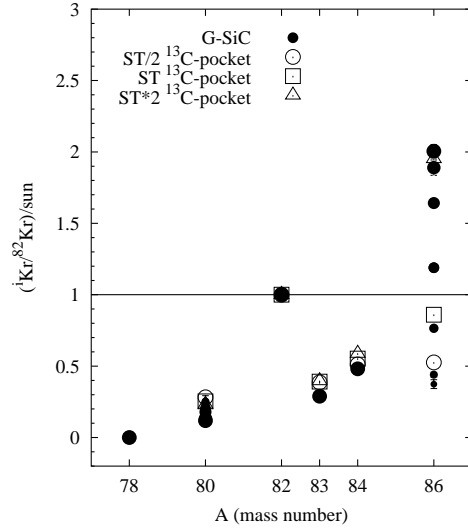


**Fig. 2.**  $M = 1.5 M_\odot$   $[\text{Fe}/\text{H}] = -0.30$ . Kr–S isotopic ratios in mainstream SiC grains (black circles) are compared with the  $s$ –component predictions at the last thermal pulse (19<sup>th</sup> TP). Predictions are presented for standard  $^{13}\text{C}$ –pockets (ST, empty squares), ST\*2 (empty triangles) and ST/2 (empty circles).

the pure  $s$ –process material present after the last third dredge–up event (see also Pignatari et al. 2004). In Fig. 2 we report the Kr–S isotopic ratios at the last thermal pulse (19<sup>th</sup> TP) for an AGB star with initial mass  $M = 1.5 M_\odot$ ,  $[\text{Fe}/\text{H}] = -0.30$ . Three  $^{13}\text{C}$ –pocket efficiencies are considered (ST, ST/2, ST\*2; see Lugaro et al. 2003) and are compared with the Kr–G observed in mainstream SiC grains. The  $(^{86}\text{Kr}/^{82}\text{Kr})_s$  ratio is strongly affected by the  $^{13}\text{C}$ –pocket efficiency and by the neutron capture channel of  $^{85}\text{Kr}$ . AGB stars with high  $^{13}\text{C}$ –pocket efficiencies can explain the high  $(^{86}\text{Kr}/^{82}\text{Kr})_G$  ratios in the coarse SiC grains, while AGB stars with low  $^{13}\text{C}$ –pocket efficiencies can explain the  $(^{86}\text{Kr}/^{82}\text{Kr})_G$  ratios in fine SiC grains. In Fig. 3 we report the Kr–S isotopic ratios predicted at the last third dredge–up episode (25<sup>th</sup> TP) for an AGB star with initial mass  $M = 3 M_\odot$ ,  $[\text{Fe}/\text{H}] = -0.30$ . From the comparison of Fig. 3 and Fig. 2, the AGB model of  $3 M_\odot$  shows a lower  $(^{80}\text{Kr}/^{82}\text{Kr})_s$  and a higher  $(^{86}\text{Kr}/^{82}\text{Kr})_s$  with re-

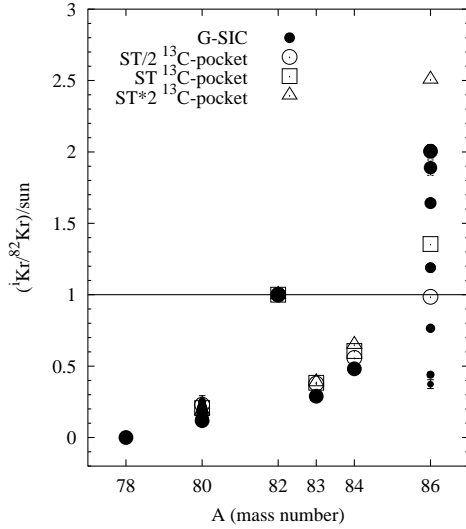


**Fig. 3.**  $M = 3 M_{\odot}$   $[\text{Fe}/\text{H}] = -0.30$ . The same as Fig. 2, but for the AGB stellar model with initial mass  $M = 3 M_{\odot}$  (last thermal pulse, 25<sup>th</sup> TP).

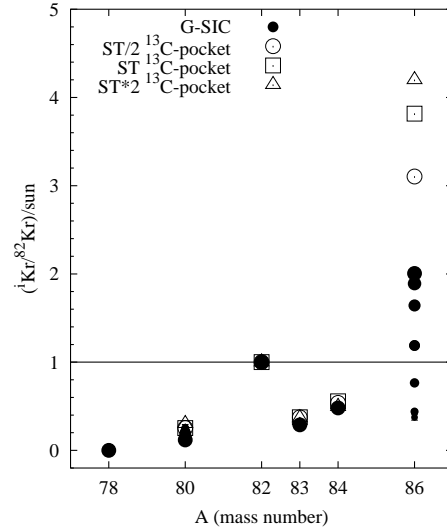


**Fig. 4.**  $M = 3 M_{\odot}$   $[\text{Fe}/\text{H}] = -0.52$ . The same as Fig. 3, but for the AGB stellar model with initial metallicity  $[\text{Fe}/\text{H}] = -0.52$  (last thermal pulse, 25<sup>th</sup> TP).

spect to the  $1.5 M_{\odot}$  case, considering the same metallicity and  $^{13}\text{C}$ -pocket efficiency. A scenario which may explain the  $(^{86}\text{Kr}/^{82}\text{Kr})_{\text{G}}$  and  $(^{80}\text{Kr}/^{82}\text{Kr})_{\text{G}}$  anticorrelation is that AGB stars with an initial mass of  $3 M_{\odot}$  produce coarse SiC grains, whereas AGB stars with an initial mass of  $1.5 M_{\odot}$  produce fine SiC grains. In Fig. 4 we report the Kr–S isotopic ratios predicted at the last third dredge–up episode (25<sup>th</sup> TP) for an AGB star with initial mass  $M = 3 M_{\odot}$ ,  $[\text{Fe}/\text{H}] = -0.52$ . The predicted  $(^{86}\text{Kr}/^{82}\text{Kr})_{\text{G}}$  ratio is too high with respect to SiC grains observations. This means that, for metallicities  $\leq 1/3 Z_{\odot}$ , the Kr–S predictions in the hot implantation scenario do not reproduce any more the Kr–G component, in agreement with the results obtained for Xe–G (Pignatari et al. 2004) and with the analysis of the Si isotopic ratios (Zinner et al. 2006). In Fig. 5 we report our predictions for the  $s$ -component at the last third dredge–up event, as weighted mass average over different masses and metallicities and over different  $^{13}\text{C}$ -pocket efficiencies. The mean  $(^{83}\text{Kr}/^{82}\text{Kr})_{\text{s}}$  and  $(^{84}\text{Kr}/^{82}\text{Kr})_{\text{s}}$  ratios are consistent with the observations within  $2\sigma$ . In this average, the predicted  $(^{80}\text{Kr}/^{82}\text{Kr})_{\text{s}}$  appears

to better reproduce fine SiC grains than coarse grains. To analyse the G–component in the framework of the cold implantation scenario, we extrapolated the  $s$ -component in the mass losing envelope for  $(\text{C}/\text{O})_{\text{env}} > 1$  and calculated a mass weighted average. In Fig. 6 we report our predictions for the cold G component of an AGB star with initial mass  $M = 1.5 M_{\odot}$ ,  $[\text{Fe}/\text{H}] = -0.30$  and ST\*2, ST, ST/2  $^{13}\text{C}$ -pockets. Here we see that the  $(^{80}\text{Kr}/^{82}\text{Kr})_{\text{G}}$  is not well reproduced in the cold implantation scenario.

#### 4.1. Main uncertainties in the predicted isotopic ratios

The  $^{80}\text{Kr}/^{82}\text{Kr}$  ratio is mainly affected by the  $^{79}\text{Se}$  branching point, as discussed in §2. The  $^{79}\text{Se}(n,\gamma)$  cross section has only a theoretical estimate and its  $\beta^{-}$ -decay rate is uncertain by a factor of two. Changing by 50% the  $(n,\gamma)$  cross section or the  $\beta^{-}$ -decay rate in the two cases  $M = 1.5, 3 M_{\odot}$ ,  $[\text{Fe}/\text{H}] = -0.30$ , ST case, the  $^{80}\text{Kr}$  abundance varies by 29% and 16%, re-

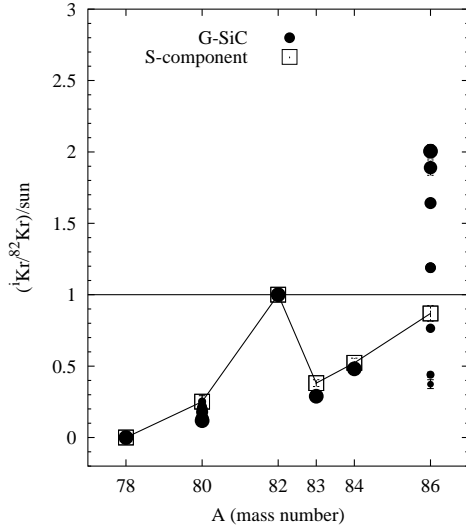


**Fig. 5.** Kr–G isotopic ratios in mainstream grains (black circles) compared with our predictions for the hot G component (open squares). Predictions are weighted mass averages over AGB models of different mass and metallicity and different  $^{13}\text{C}$ -pockets ( $M = 1.5 M_{\odot}$  [ $\text{Fe}/\text{H} = -0.30, -0.52$ ;  $M = 3 M_{\odot}$  [ $\text{Fe}/\text{H} = 0, -0.30$ ; ST\*2–ST/12  $^{13}\text{C}$ -pockets]). Error bars of theoretical predictions take into account the uncertainty of the Mutti et al. (2005) cross sections.

spectively. The  $^{79}\text{Se}$  branching has only small effects on  $^{82}\text{Kr}$ –S.

The  $(^{86}\text{Kr}/^{82}\text{Kr})_s$  ratio is strongly affected by the  $^{85}\text{Kr}$  branching point. The  $^{85}\text{Kr}(n,\gamma)$  cross section has a quite large uncertain theoretical evaluation. Changing by a factor of two the  $^{85}\text{Kr}(n,\gamma)$  cross section in the  $M = 1.5 M_{\odot}$  [ $\text{Fe}/\text{H} = -0.30$ , ST case, the  $^{86}\text{Kr}/^{82}\text{Kr}$  predicted ratio varies by 80%. The  $^{86}\text{Kr}/^{82}\text{Kr}$  ratio is also affected by the main  $s$ -process neutron sources: by  $^{13}\text{C}(\alpha,n)^{16}\text{O}$  and by  $^{22}\text{Ne}(\alpha,n)^{25}\text{Mg}$  (see Pignatari et al. 2005b for details). The other  $^i\text{Kr}/^{82}\text{Kr}$  isotopic ratios are only slightly affected by the above uncertainties. To conclude, it is difficult to obtain a well established estimate for the  $^{86}\text{Kr}/^{82}\text{Kr}$  ratio from AGB models, and at least a factor of two of uncertainty has to be taken into account.

## 5. Conclusions

We compared the krypton G component implanted in mainstream SiC grains with AGB model predictions for different masses, metallicities and  $^{13}\text{C}$ -pocket efficiencies. We confirm a scenario where mainstream SiC grains form in low mass AGB stars ( $M = 1.5\text{--}3 M_{\odot}$ ) with solar-like metallicity and a spread of  $^{13}\text{C}$ -pocket efficiencies. Comparison of predicted and observed  $(^{80}\text{Kr}/^{82}\text{Kr})_G$  ratios confirms that krypton is mainly implanted into SiC grains by a hot ionised wind, probably in the PPN–PN phases. The predicted  $(^{86}\text{Kr}/^{82}\text{Kr})_s$  isotopic ratio is strongly affected by the nuclear uncertainty of the unstable  $^{85}\text{Kr}$  neutron capture cross section. A different implantation energy of  $^{86}\text{Kr}$  and  $^{82}\text{Kr}$  can only partially explain the  $(^{86}\text{Kr}/^{82}\text{Kr})_G$  spread observed in SiC grains of different sizes. On the other hand, we showed that the  $(^{86}\text{Kr}/^{82}\text{Kr})_G$  spread is predicted considering different initial star masses and different  $^{13}\text{C}$ -pocket efficiencies, as well as

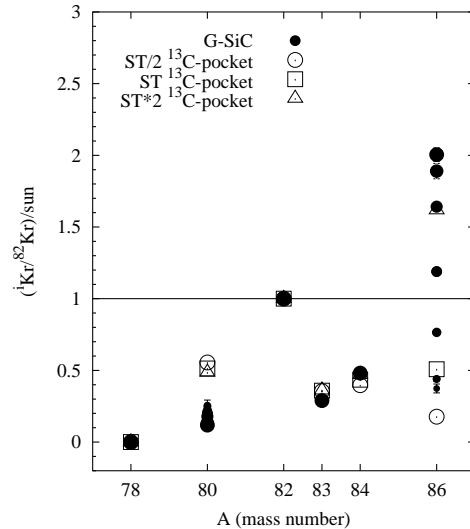


**Fig. 6.**  $M = 1.5 M_{\odot}$  [ $\text{Fe}/\text{H} = -0.30$ , ST\*2, ST, ST/2  $^{13}\text{C}$ -pockets]. Kr–G isotopic ratios in mainstream SiC grains (black circles) compared with our predictions for the cold G component (open squares). Predictions are weighted average abundances in the winds with  $(\text{C}/\text{O})_{\text{env}} > 1$ .

the anticorrelation between  $(^{80}\text{Kr}/^{82}\text{Kr})_{\text{G}}$  and  $(^{86}\text{Kr}/^{82}\text{Kr})_{\text{G}}$ . A tentative reproduction of the Kr isotopic compositions in mainstream SiC grains is to attribute the fine grains to AGB stars of  $1.5 M_{\odot}$  and coarse grains to AGB stars of  $3 M_{\odot}$ , both of solar-like metallicity.

This idea can be tested with measurement of other s-process elements whose isotopic compositions are sensitive to branches in the s-process path, such as Zr.

*Acknowledgements.* Part of this work was supported by the Italian PRIN2004-025729004 Project *Nucleosynthesis in low and intermediate mass stars: crucial tests from early evolutionary phases of the Galaxy and of the Solar System*. This work was also partially supported by the U.S. National Aeronautics and Space Administration. Thanks the Aspen Center for Physics for insightful discussions relating to this work during the *Summer School on the s-process* organised by R. Reifarth and F. Herwig.

## References

- Arlandini, C., Käppeler, F., Wisshak, K., Gallino, R., Lugaro, M., Busso, M., Straniero, O. 1999, *ApJ* 525, 886
- Bao, Z. Y., Beer, H., Käppeler, F., Voss, F., Wisshak, K., Rauscher, T. 2000, *ADNDT* 76, 70
- Gallino, R., Busso, M., Picchio, M., Raiteri, C.M. 1990, *Nature* 348, 298
- Gallino, R., Arlandini, C., Busso, M., Lugaro, M., Travaglio, C., Straniero, O., Chieffi, A., Limongi, M. 1998, *ApJ* 497, 388
- Klay, N., Käppeler, F. 1988, *Phys. Rev. C* 38, 295
- Lewis, R.S., Amari, S., Anders E. 1990, *Nature* 348, 293
- Lewis, R.S., Amari, S., Anders E. 1994, *Geochim. Cosmochim. Acta* 58, 471
- Lodders, K. 2003, *ApJ* 591, 1220
- Lugaro, M., Davis, A.M., Gallino, R., Pellin, M.J., Straniero, O., Käppeler, F. 2003, *ApJ* 593, 486
- Mutti, P., Beer, H., Brusegan, A., Corvi, F., Gallino, R. 2005, in *International Conference on Nuclear Data for Science and Technology*, AIP Conf. 769, 1327
- Pignatari, M., Gallino, R., Straniero, O., Davis, A. 2004, *Mem. SAI* 75, 729
- Pignatari, M., Gallino, R., Baldovin, C., Herwig, F. 2005a, in *IAU Symposium 228*, edited by Hill, V.; Franois, P.; Primas, F., Cambridge University Press, pp.495-496
- Pignatari, M., Gallino, R., Käppeler, F., Wiescher, M. 2005b, *Nucl. Phys. A* 758, 451
- Straniero, O., Chieffi, A., Limongi, M., Busso, M., Gallino, R., Arlandini, C. 1997, *ApJ* 478, 332
- Verchovsky, A.B., Wright, I.P., Pillinger, C.T. 2004, *ApJ* 607, 611
- Ward, R.A., Newman, M.J., Clayton, D.D. 1976, *ApJS* 31, 33
- Zinner, E. 1998, *AREPS* 26, 147
- Zinner, E., Nittler, L.R., Gallino, R., Karakas, A.I., Lugaro, M., Straniero, O., Lattanzio, J.C. 2006, *ApJ Supplement*, accepted